Spectroscopy of diatomic ZrF and ZrCl: 760 – 555 nm

Alonzo Martinez and Michael D. Morse[a)]
Department of Chemistry, University of Utah, Salt Lake City, Utah 84112, USA

(Received 21 April 2011; accepted 13 June 2011; published online 12 July 2011)

The optical spectrum of diatomic ZrF has been investigated, with transitions recorded in the range from 14 700 to 18 000 cm^{-1}. Many bands have been observed, several of which can be grouped into three band systems. Rotationally resolved investigations are hampered by perturbations that are rampant among the excited states, but three unperturbed bands have revealed that the ground state of ZrF has $\Omega'' = 3/2$, with a bond length of $r_e'' = 1.854(1)$ Å. Hot bands originating from $v'' = 1$ provide the ground state vibrational interval, $\Delta G_{1/2}'' = 691.45(2)$ cm^{-1} for $^{90}Zr^{19}F$. Based on comparisons to ZrCl and ligand-field considerations, the ZrF ground state is assigned as a $^2\Delta_{3/2}$ level deriving from the $3\sigma^2\ 1\delta^1$ configuration, in agreement with a previous study. In addition to the measurements on ZrF, vibronically resolved spectra of ZrCl have been recorded over the 13 000 to 18 000 cm^{-1} range, and four band systems have been identified. © *2011 American Institute of Physics*. [doi:10.1063/1.3608055]

I. INTRODUCTION

The spectroscopy of the diatomic transition metal halides has been investigated since the early days of molecular spectroscopy. In the past 50 years enormous progress has been made, with the result that the ground and at least some of the low-lying electronic states are now known for all of the 3*d* series of transition metal fluorides (MF) and chlorides (MCl), and progress is being made for the 3*d* bromides and iodides. In contrast, the electronic structure of the 4*d* MF and MCl molecules remains poorly known, with experimental spectra available only for YF,[1] YCl,[2] ZrF,[3] ZrCl,[4–7] NbCl,[8] RuF,[9] RhF,[10] RhCl,[11] AgF,[12] and AgCl.[13] While the nature of the halogen (F *vs.* Cl) makes no difference in the ground electronic state for the 3*d* metal halides, there is an interesting dependence of the ground electronic configuration and term on whether the metal atom comes from the 3*d* or 4*d* series. Thus, for example, the ground states of TiF and TiCl ($\sigma^1\delta^1\pi^1$, $^4\Phi_r$) (Refs. 14 and 15) differ from that of their isovalent 4*d* congeners, ZrF and ZrCl($\sigma^2\delta^1$, $^2\Delta_r$).[3,7] Likewise, the ground states of the group 8 halides FeF ($\sigma^1\delta^3\pi^2\sigma^1$, $^6\Delta_i$) (Ref. 16) and RuF ($\sigma^1\delta^3\pi^3$, $^4\Phi_i$)[9] differ, as do those of the group 9 halides CoF and CoCl ($\sigma^2\delta^3\pi^3$, $^3\Phi_i$) (Refs. 17 and 18) and RhF and RhCl ($\sigma^1\delta^4\pi^3$, $^3\Pi_i$).[10,11] These differences reflect the variations in n*d* *vs.* (n+1)*s* orbital sizes, energies, and occupation numbers that occur as one moves down a column within the transition metal series.

Despite the electronic complexity of the diatomic transition metal halides, high-quality *ab initio* calculations have been reported on a large number of low-lying electronic states for all of the 3*d* MF molecules.[19–21] Fewer detailed computational investigations of the 4*d* series have been reported, however, with most of the species investigated using density functional methods.[22,23] Generally, these density functional studies only report the lowest energy state of a given spin multiplicity. The ground state of ZrF has been calculated to be a $^2\Delta$ state, deriving from the $3\sigma^2\ 1\delta^1$ configuration in both density functional theory[23] and in *ab initio* calculations.[24] In a more recent density functional calculation, however, the ground state is predicted to be of quartet multiplicity.[22] In the most recent calculations on ZrF, internally contracted multireference configuration interaction (IC-MRCI) calculations predict a $3\sigma^2\ 1\delta^1$, $^2\Delta$ ground term, followed by the $3\sigma^1\ 1\delta^2$, $^4\Sigma^-$ term at $T_0 = 2383$ cm^{-1} and the $3\sigma^1\ 1\delta^1\ 2\pi^1$, $^4\Phi$ term at $T_0 = 4179$ cm^{-1}.[3] A complementary computational method that has shown great promise for the study of diatomic metal halides is ligand field theory (LFT),[25,26] which has been used to effectively treat entire manifolds of states in studies of the lanthanide halides[27–29] and oxides,[30–32] the actinide molecules ThO and UO,[33] the alkaline earth halides, oxides, and hydroxides,[34–36] and the transition metal oxides[37,38] and halides.[39–43] Ligand field methods show good promise for systematically understanding the differences between the electronic structures of the 3*d* *vs.* 4*d* metal halides.

Early reports of the spectra of ZrF (Ref. 44) were subsequently shown to arise from CuF.[45] After the initial submission of this report, we became aware of a nearly contemporaneous study of ZrF in the 420-470 nm range.[3] That investigation is in agreement with the present study, demonstrating that the ground state of ZrF has $\Omega = 3/2$, arising from the $3\sigma^2\ 1\delta$, $^2\Delta_{3/2}$ term. In one other previous investigation, the bond energy of ZrF has been evaluated through high-temperature mass spectrometric measurements of the gaseous equilibrium

$$BaF(g) + Zr(g) \leftrightarrow Ba(g) + ZrF(g), \tag{1.1}$$

providing a value of $D_{298}^0(Zr-F) = 6.49 \pm 0.20$ eV.[46] The appearance potential of ZrF^+ from ZrF neutral molecules has been measured as 6.5±0.5 eV in the same study.[46]

Although the spectra of ZrF are not well-known, a larger number of studies of ZrCl have been reported.[4,5,7,47] Initial work began in 1961, when Carroll and Daly reported three band systems in the ultraviolet that were suggested to arise from a $^4\Sigma^-$ ground state.[47] A reinvestigation of the band

a)Electronic mail: morse@chem.utah.edu. FAX: (801) 581-8433.

system near 410 nm maintained the assignment as a $^4\Pi \leftarrow X^4\Sigma^-$ transition, although the rotational lines were not resolved.[4] Another band system was identified in the near infrared in 1980, and was rotationally resolved and assigned as a parallel transition. It was thought to be a $^2\Pi - ^2\Pi$ system, although $^2\Delta - ^2\Delta$ and $^2\Phi - ^2\Phi$ transitions were also consistent with the data.[48] More recently, ZrCl has been investigated in a series of Fourier transform emission studies, and additional band systems have been observed.[5–7] The ground state has now been assigned as $X^2\Delta_r$, deriving from a $\sigma^2\ \delta^1$ configuration of the Zr^+ ion,[7] based largely on the results of *ab initio* calculations.[7,49] The complexity of the electronic structure of ZrCl (or ZrF) arises because of the large number of low-lying states that result from the $5s^2\ 4d^1$, $5s^1\ 4d^2$, and $4d^3$ configurations of the Zr^+ ion. This leads to at least 19 Hund's case (a) Λ-S states lying within 15 000 cm^{-1} of the ground state.[7]

Having recently investigated the electronic structure of YF,[50] our intention in this paper is to shed some light on the electronic structure of its neighbor, ZrF. In the process, we have been able to determine the ground state bond length, vibrational frequency, and Ω value, and have identified several excited states.

II. EXPERIMENTAL

Diatomic ZrF was investigated by resonant two-photon ionization (R2PI) spectroscopy in a jet-cooled molecular beam with time-of-flight mass spectrometric detection, using an instrument that has been previously described.[51] The molecule was produced by pulsed laser ablation (Nd:YAG, 532 nm) of a zirconium sample disk in the throat of a supersonic expansion of helium containing about 0.1% CCl_2F_2 or less. The resulting supersonic beam was roughly collimated with a 1 cm diameter conical skimmer and admitted into the Wiley-McLaren[52] ion source region of a reflectron time-of-flight mass spectrometer.[53] In the ion source region the output of a Nd:YAG-pumped dye laser was counterpropagated along the molecular beam axis and this axis was intersected at right angles with the output of an excimer laser in order to produce ions. Initial experiments were undertaken using ArF excimer radiation (193 nm, 6.42 eV). At high ArF fluences, the isotopes of Zr, ZrN, ZrO, ZrF, ZrCl were readily observed, and the alignment of the lasers into the chamber was optimized using a known transition in ZrN.[54] The ZrN signal decayed over time as the surface layers of the zirconium sample were removed.

Initial scans were conducted using ArF (193 nm, 6.42 eV) radiation for the ionizing photon, but only a few transitions could be observed in ZrF, presumably due to efficient two-photon ionization at 193 nm, leading to a high background signal. This suggests that the ArF wavelength is resonant with a molecular transition, perhaps terminating on a Rydberg level. Nevertheless, the observation of transitions using ArF excimer radiation for ionization places the ionization energy of ZrF above 6.42 eV. When the ionization laser was changed to KrF (248 nm, 5.00 eV), the resonance enhancement was greatly improved. After this was discovered, all subsequent scans were undertaken using KrF excimer radiation as the ionizing photon. Because the molecule used as a source of fluorine was CCl_2F_2, we simultaneously recorded the spectra of ZrCl. In this article we report only the results of the vibrationally resolved study of ZrCl, however, focusing instead on vibrationally and rotationally resolved studies of ZrF.

Vibronic scans were conducted over the range 12 500 – 18 000 cm^{-1}, and were calibrated using atomic transitions of zirconium that were observed over this range, many of which originated from metastable Zr atoms.[55] To achieve rotational resolution, selected bands were examined using an intracavity etalon to narrow the linewidth (~0.04 cm^{-1}). Under these conditions, the laser was pressure-scanned using SF_6. The rotationally resolved scans were calibrated by simultaneously recording the transmission spectrum through a cell filled with I_2 vapor, using the known I_2 absorption lines as tabulated by Gerstenkorn and Luc,[56] corrected for the error in the original measurements[57] and for the Doppler shift of the ZrF molecules as they traveled toward the light source at the beam velocity of helium (1.77×10^5 cm s^{-1}). The Doppler correction amounted to +0.10 cm^{-1} or less for all of the bands investigated.

Excited state lifetimes were also measured for many of the observed bands by firing the excimer laser at the time of maximum ZrF density, but varying the timing of the dye laser pulse. By monitoring the ion signal as a function of the delay between the two laser pulses and fitting the resulting decay curve to an exponential model using the Marquardt nonlinear least-squares algorithm,[58] the 1/e decay time, τ, was measured. To obtain an estimate of the error in this quantity, the decay curve was recorded and fitted a minimum of 4 times. The mean of the fitted lifetimes is reported, along with the standard deviation for the set of fitted values.

III. RESULTS

A. Low resolution spectra of ZrF and ZrCl

All together, 93 vibronic transitions were observed in the low resolution spectrum of $^{90}Zr^{19}F$ over the range 14 500 to 18 000 cm^{-1}, of which 26 were ultimately arranged into three band systems. A portion of the spectrum covering the 15 500-16 500 cm^{-1} range is displayed in Figure 1. In order to determine whether vibrational hot bands were present, the wavenumber difference between all pairs of features was computed, and a Gaussian function with a width of 1 cm^{-1} was assigned to each wavenumber difference. The resulting 4,278 Gaussian functions were summed to create a continuous function representing a histogram of the wavenumber differences, with the idea that repeated differences would sum in phase to provide a peak in the plot. The resulting band difference histogram for $^{90}Zr^{19}F$ is displayed in Figure 2. Only a single peak is observed, at 691.34 cm^{-1}. The fact that there are multiple occurrences of band differences that match this value strongly suggests that the $v'' = 1$ level of the ground state is populated in the molecular beam, and the $\Delta G''_{1/2}$ value for ground state $^{90}Zr^{19}F$ is 691.34 cm^{-1}. Repeating this procedure for the $^{91}Zr^{19}F$, $^{92}Zr^{19}F$, and $^{94}Zr^{19}F$ isotopic modifications also provided peaks shifted to the slightly lower frequencies of 690.56, 689.98, and 688.72 cm^{-1}, in keeping with the

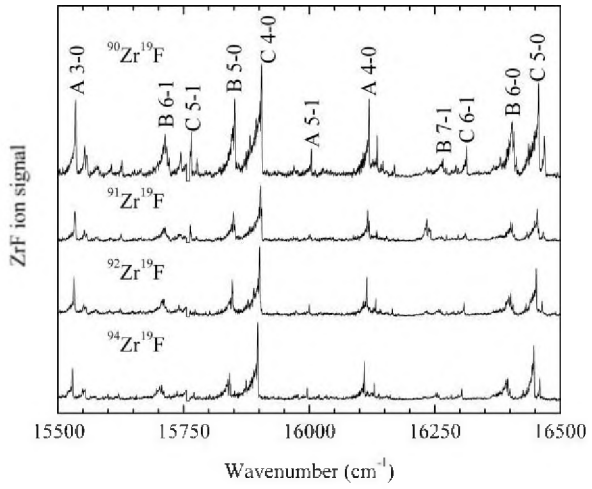

FIG. 1. A portion of the spectrum recorded for the various isotopomers of ZrF, labeled according to the assigned band systems.

larger reduced masses of the heavier isotopic modifications. A more precise value of $\Delta G''_{1/2}$ is provided below from rotationally resolved studies.

Next, bands were sought that could be grouped into band systems, assuming near-constant intervals between successive bands in a progression and isotope shifts, $\nu(^{90}Zr^{19}F) - \nu(^{94}Zr^{19}F)$, that increased with increasing v'. Four progressions were readily assigned, although one of these turned out to be a set of $v'' = 1$ hot bands built on one of the other progressions. Vibrational assignments were established by varying the assignment of v', fitting the measured bands to obtain values of ω_e', $\omega_e'x_e'$, T_0, and $\Delta G''_{1/2}$, and then computing the transition wavenumber as a function of a continuous parameter, v', using the equation

$$v = T_0 + v'\,\omega'_e - (v'^2 + v')\,\omega'_e x'_e. \qquad (3.1)$$

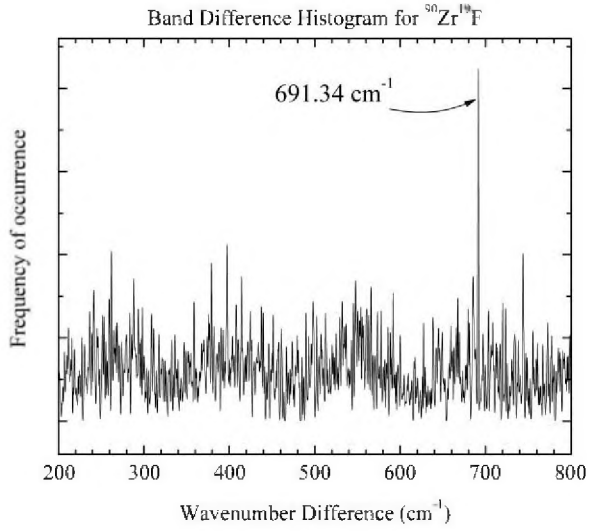

FIG. 2. Band difference histogram plot for $^{90}Zr^{19}F$, showing a single peak at 691.34 cm^{-1}. This interval is assigned as the $\Delta G''_{1/2}$ value for the ground electronic state of $^{90}Zr^{19}F$.

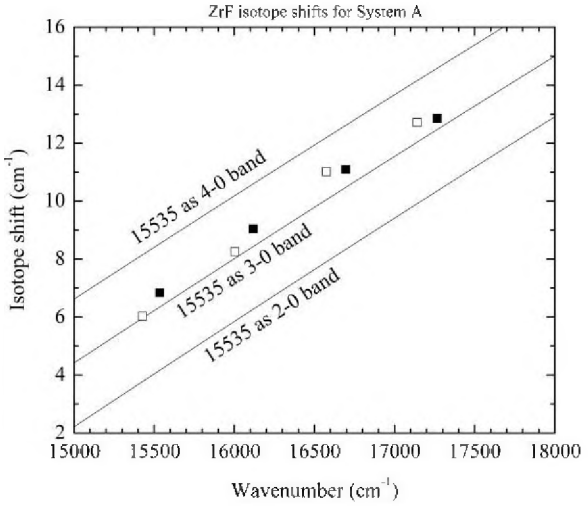

FIG. 3. Calculated and measured isotope shifts for the A System of ZrF, for various possible vibrational numberings. Cold bands originating from $v'' = 0$, are indicated by the filled squares, while hot bands originating from $v' = 1$ are indicated by open squares. From this plot it is clear that the first band observed in the progression, at 15 535 cm^{-1}, is the 3-0 band.

The corresponding isotope shift was calculated as a function of v', as

$$\nu(^{90}Zr^{19}F) - \nu(^{94}Zr^{19}F) = (1-\rho)[\omega'_e(v' + 1/2) - \omega''_e(1/2)] - (1-\rho^2)[\omega'_e x'_e(v' + 1/2)^2 - \omega''_e x''_e(1/2)^2]. \qquad (3.2)$$

Here, the $^{90}Zr^{19}F$ isotope was used as the reference species, and the fitted values of ω_e', $\omega_e'x_e'$, T_0, and $\Delta G''_{1/2}$, which is taken to equal ω''_e, were used in Eqs. (3.1) and (3.2). For purposes of calculating the isotope shift, it was assumed that $\omega_e''x_e''$ is zero. The parameter, ρ, is given by $[\mu(^{90}Zr^{19}F)/\mu(^{94}Zr^{19}F)]^{1/2}$.[59] Plots of the resulting isotope shift *vs.* transition wavenumber provided a definite vibrational numbering for all three band systems, as illustrated in Figure 3 for the A-X system. The bands that have been arranged into band systems are listed in Table I, while the remaining band positions, along with band difference histograms, isotope shift plots, band positions and isotope shift plots for ZrCl, and rotational line positions and fits for ZrF, are available in the supplementary material[60] and also from the author (M.D.M.). This document also provides figures that display vibrationally (ZrF and ZrCl) and rotationally resolved spectra (ZrF only).

Similarly, 75 bands were observed in $^{90}Zr^{35}Cl$ (38.98% natural abundance), which falls at mass 125. Due to the presence of two naturally occurring isotopes of chlorine, the remaining prominent features in the mass spectrum of ZrCl are mixed isotopomers, but mass 129 is approximately 76% $^{94}Zr^{35}Cl$ and 24% $^{92}Zr^{37}Cl$. We have assigned vibronic features for $^{94}Zr^{35}Cl$ in this mass channel to the corresponding bands in the pure isotopomer, $^{90}Zr^{35}Cl$. Although not as clean as in the case of ZrF, the measured isotope shifts provide a convincing vibrational assignments for the four band systems identified for ZrCl. These are listed in Table II. Again, a listing of all the measured bands in mass 125 ($^{90}Zr^{35}Cl$) and mass 129 (76% $^{94}Zr^{35}Cl$ + 24% $^{92}Zr^{37}Cl$) are provided in the supplementary documents. It is likely that the upper states

TABLE I. Band heads and excited state lifetimes of assigned bands of ZrF.[a]

Band	$^{90}Zr^{19}F$	$^{91}Zr^{19}F$	$^{92}Zr^{19}F$	$^{94}Zr^{19}F$	Isotope shift $\nu(^{90}Zr^{19}F)$-$\nu(^{94}Zr^{19}F)$	Lifetime (μs)
A - X 3-0	15 535.4(−0.1)	15 533.9(0.3)	15 531.9(−0.1)	15 528.6(0.0)	6.84	
A - X 4-0	16 118.9(0.4)	16 116.5(−0.2)	16 114.3(0.5)	16 109.8(0.2)	9.04	2.03(2)
A - X 5-0	16 695.6(0.0)	16 692.8(−0.1)	16 689.9(0.0)	16 684.6(0.0)	11.09	
A - X 6-0	17 266.4(−0.4)		17 259.7(−0.4)	17 253.6(−0.2)	12.85	
A - X 3-1	14 844.0(−0.3)	14 843.0(−0.5)	14 841.8(−0.3)	14 839.6(−0.3)	4.40	
A - X 4-1	15 427.7(0.4)	15 427.2(0.8)	15 424.3(0.3)	15 421.2(0.4)	6.03	
A - X 5-1	16 004.2(−0.2)	16 002.2(−0.5)	15 999.9(−0.1)	15 995.9(0.1)	8.25	
A - X 6-1	16 575.5(−0.2)	16 572.4(0.2)	16 569.9(−0.3)	16 564.5(−0.5)	11.01	
A - X 7-1	17 141.3(0.3)		17 135.0(0.4)	17 128.6(0.3)	12.71	
B - X 5-0	15 851.9(−0.2)	15 849.6(−1.0)	15 846.7(−1.2)	15 841.8(−0.4)	10.15	1.51(8)
B - X 6-0	16 407.6(−0.9)	16 404.5(1.7)	16 401.2(0.7)	16 395.0(1.1)	12.53	1.20(5)
B - X 7-0	16 957.8(1.1)	16 954.2(−0.7)	16 950.3(0.6)	16 943.2(−0.6)	14.64	0.90(2)
B - X 5-1	15 160.5(1.4)	15 158.9(0.4)	15 157.7(1.2)	15 153.1(0.4)	7.39	
B - X 6-1	15 712.9(−2.6)	15 710.3(−0.4)	15 708.4(−0.7)	15 703.2(−1.1)	9.75	
B - X 7-1	16 266.1(2.4)		16257.7(−0.6)	16 254.9(0.6)	11.22	
B - X 8-1	16 802.8(-1.1)					
C - X 2-0	14 784.9(−0.2)	14 782.8(−0.6)	14 781.3(−0.6)	14 780.0(−0.4)	4.85	
C - X 3-0	15 347.3(0.0)	15 346.3(0.7)	15 344.7(0.8)	15 341.9(0.4)	5.41	0.36(1)
C - X 4-0	15 905.2(0.6)	15 903.1(0.4)	15 901.0(0.4)	15 897.8(0.5)	7.44	0.49(3)
C - X 5-0	16456.4(−0.5)	16 454.0(−0.6)	16 451.5(−0.6)	16 447.1(−0.6)	9.37	0.42(2)
C - X 6-0	17 004.3(0.1)	17 001.1(−0.3)	16 998.0(−0.3)	16 992.4(−0.3)	11.86	0.49(1)
C - X 7-0	17 546.5(−0.1)	17 543.3(0.3)	17 539.5(0.3)	17 532.6(0.2)	13.95	0.47(1)
C - X 4-1	15 213.8(0.4)	15 212.8(0.6)	15 211.1(0.1)	15 208.8(0.0)	4.96	
C - X 5-1	15 765.3(−0.4)	15 763.4(−0.7)				0.43(2)
C - X 6-1	16 312.8(−0.3)	16 310.8(−0.1)	16 308.3(−0.3)	16 304.0(−0.2)	8.84	
C - X 7-1	16 855.8(0.3)	16 852.6(0.1)	16 849.7(0.2)	16 844.0(0.1)	11.83	

Fitted spectroscopic constants

System	Parameter	$^{90}Zr^{19}F$	$^{91}Zr^{19}F$	$^{92}Zr^{19}F$	$^{94}Zr^{19}F$
A – X	T_0	13 751.1(1.9)	13 744.2(4.7)	13 751.6(2.0)	13750.5(1.8)
	ω_e'	606.55(0.91)	610.0(2.5)	605.1(1.0)	604.5(0.9)
	$\omega_e'x_e'$	2.94(0.09)	3.38(0.25)	2.91(0.09)	2.94(0.08)
	$\Delta G''_{1/2}$	691.15(0.27)	690.20(0.50)	689.88(0.29)	688.77(0.26)
B – X	T_0	12 949.4(38.9)	13 046.1(58.2)	13 033.9(46.5)	13 058.5(41.7)
	ω_e'	604.8(13.4)	568.6(21.7)	573.0(17.0)	561.9(15.3)
	$\omega_e'x_e'$	4.03(0.97)	1.29(1.69)	1.70(1.31)	0.85(1.17)
	$\Delta G''_{1/2}$	693.0(1.9)	692.4(1.8)	691.5(1.2)	689.6(1.1)
C – X	T_0	13 645.83(1.23)	13 643.50(1.75)	13 641.95(1.70)	13 642.03(1.33)
	ω_e'	577.07(0.62)	577.68(0.89)	577.89(0.87)	577.21(0.68)
	$\omega_e'x_e'$	2.48(0.06)	2.58(0.08)	2.64(0.09)	2.68(0.06)
	$\Delta G''_{1/2}$	691.12(0.31)	690.50(0.44)	689.68(0.45)	688.50(0.35)

[a]All entries except the lifetime are given in wavenumbers (cm^{-1}). Following each transition wavenumber listed, the residual in the fit (observed - calculated) is provided in parentheses. Likewise, the 1σ error limits in the fitted constants are provided in parentheses following each entry.

labeled A and E, with T_0 values of 14 363 and 13 967 cm^{-1}, respectively, correspond to the calculated $2\,^2\Phi_{5/2}$ and $3\,^2\Pi_{1/2}$ states,[7] which neglecting spin-orbit interaction are calculated to lie at 12 315 and 11 108 cm^{-1}, respectively. To confirm this conjecture would require rotationally resolved studies to determine the Ω values of the upper states of these transitions.

B. Rotationally resolved spectra of ZrF

In order to measure the ZrF bond length and gain insight into the electronic symmetries of the ground and excited electronic states, experiments were undertaken to rotationally resolve bands belonging to the three band systems. The 3-0 and 4-0 bands of the A-X system were successfully resolved and analyzed, as was the 4-0 band of the C-X system. The remaining bands that were investigated (the 5-0, 6-0, and 7-0 bands of the B-X system, and the 5-0, 5-1, and 6-0 bands of the C-X system) were all perturbed by nearby states. In some cases, line assignments could be made using the ground state rotational constant obtained from the unperturbed bands and combination differences, but this was not always possible. From the fits of the unperturbed 3-0 and 4-0 bands of the A-X system, the fit of the 4-0 band of the C-X system, and one unperturbed *e/f* component of the 6-0 band of the C-X system, a simultaneous fit of the rotational lines provides ground and excited state rotational constants and bond lengths as listed in Table III.

Using only data from the better-determined isotopic modifications, $^{90}Zr^{19}F$, $^{91}Zr^{19}F$, and $^{92}Zr^{19}F$, this gives a weighted

TABLE II. Band heads of assigned bands of ZrCl.[a]

Band	$^{90}Zr^{35}Cl$	$^{94}Zr^{35}Cl$	Isotope shift $\nu(^{90}Zr^{35}Cl)$-$\nu(^{94}Zr^{35}Cl)$
A - X 2-0	15023.1(2.4)	15020.5(3.2)	2.6
A - X 3-0	15347.9(−3.5)	15340.4(−4.7)	7.5
A - X 4-0	15683.4(−0.1)	15675.8(0.6)	7.6
A - X 5-0	16018.1(1.2)	16008.5(0.9)	9.6
A - X 3-1	14936.4(−1.9)	14931.6(−2.7)	4.8
A - X 4-1	15272.1(1.7)	15266.7(2.3)	5.4
A - X 5-1	15605.9(2.1)	15599.3(2.6)	6.6
A - X 6-1	15936.7(−1.9)	15929.0(−2.3)	7.7
B - X 0-0	15648.6(0.0)	15648.7(0.0)	−0.1
B - X 1-0	15973.2(0.0)	15971.4(0.0)	1.8
B - X 2-0	16295.7(0.1)	16292.2(0.2)	3.5
B - X 3-0	16615.8(0.0)	16610.4(−0.3)	5.4
B - X 4-0	16933.8(0.0)	16927.5(0.1)	6.3
B - X 4-1	16521.9(0.0)	16519.0(0.0)	2.9
E - X 0-0	13967.4(0.0)	13968.2(0.0)	−0.8
E - X 1-0	14320.2(−0.4)	14319.2(0.0)	1.0
E - X 2-0	14670.7(0.4)	14667.2(0.0)	3.5
E - X 1-1	13912.6(0.4)	13913.3(0.0)	−0.7
E - X 2-1	14261.4(−0.4)	14261.3(0.0)	0.1
E - X 3-1	14607.9(0.0)		
C - X 0-0	17463.7	17466.0	−2.3
C - X 1-0	17809.2	17807.0	2.2
C - X 0-1	17054.3	17055.9	−1.6
C - X 0-2	16643.8	16650.6	−6.8

Fitted spectroscopic constants

System	Parameter	$^{90}Zr^{35}Cl$	$^{94}Zr^{35}Cl$
A – X	T_0	14363.2(10.6)	14368.3(13.9)
	ω_e'	326.7(6.3)	321.2(8.2)
	$\omega_e'x_e'$	−0.67(0.69)	−1.12(0.90)
	$\Delta G_{1/2}'$	413.1(2.3)	410.8(3.0)
B – X	T_0	15648.59(0.05)	15648.75(0.24)
	ω_e'	326.87(0.07)	324.59(0.35)
	$\omega_e'x_e'$	1.11(0.01)	0.98(0.07)
	$\Delta G_{1/2}''$	411.89(0.07)	408.39(0.35)
C – X	T_0	17463.7	17466.0
	$\Delta G_{1/2}''$	345.5	341.0
	ω_e''	408.3	414.9
	$\omega_e''x_e''$	−0.55	2.4
E – X	T_0	13967.4(0.6)	13968.2(0.0)
	ω_e'	356.8(1.1)	354.0(0.0)
	$\omega_e'x_e'$	1.79(0.26)	1.50(0.00)
	$\Delta G_{1/2}''$	408.5(0.6)	405.9(0.0)

[a]All entries are given in wavenumbers (cm^{-1}). Following each transition wavenumber listed, the residual in the fit (observed - calculated) is provided in parentheses. Likewise, the 1σ error limits in the fitted constants are provided in parentheses following each entry.

average bond length for the $v'' = 0$ level of the ZrF $\Omega = 3/2$ ground state of r_0 ($X\,^2\Delta_{3/2}$) = 1.8577(1) Å. In fact, this estimate of the $v'' = 0$ bond length is in error because of **S**-uncoupling interactions between the $X_1\,^2\Delta_{3/2}$ and $X_2\,^2\Delta_{5/2}$ states. A correction for this interaction can be made if we assume that the spin-orbit splitting in the $X\,^2\Delta$ state is identical to that found in ZrCl (705 cm^{-1}),[7] using the well-known formula[59]

$$B_{eff}(X_1\,^2\Delta_{3/2}) = B(1 + 2B\Sigma/A\Lambda). \quad (3.3)$$

Using this formula with $\Sigma = -1/2$ and $A\Lambda = 705$ cm^{-1}, we obtain a revised value of $r_0(X\,^2\Delta) = 1.8573(1)$ Å. Finally, combining the corrected B_0 value with a similarly corrected B_1 value obtained from a vibrational hot band, we obtain our best estimate for $r_e(X\,^2\Delta)$ of 1.854(1) Å. Unfortunately, the poor quality of the data for the vibrational hot band increases the error in this value significantly compared to the r_0 value. Here and throughout this article, 1σ error limits are provided in parentheses, in units of the last quoted digit.

1. Rotationally resolved spectra of the A3/2-X3/2 system

Figure 4 displays a rotationally resolved scan over the 3-0 band of the A-X system, as recorded for the most abundant

TABLE III. Fitted rotational constants and bond lengths of ZrF from rotationally resolved studies.[a]

Level	Spectroscopic parameter	$^{90}Zr^{19}F$	$^{91}Zr^{19}F$	$^{92}Zr^{19}F$	$^{94}Zr^{19}F$	$^{96}Zr^{19}F$
C3/2 $v' = 6$ [a]	ν_0	17002.6818(45)	16999.6208(27)	16996.6671(37)		
	B_6'	0.26837(7)	0.26813(6)	0.26839(7)		
	r_6'	2.0013(3)	2.0002(2)	1.9973(3)		
C3/2 $v' = 5$[a]	ν_0	16455.1229(81)	16452.6216(42)	16450.1862(39)	16445.5015(69)	16441.0486(69)
	B_5'	0.26441(16)	0.26414(7)	0.26393(10)	0.26348(26)	0.26373(19)
	r_5'	2.0162(6)	2.0153(3)	2.0142(4)	2.0122(10)	2.0077(7)
C3/2 $v' = 4$	ν_0	15902.5668(34)	15900.6393(24)	15898.6757(28)	15895.1678(19)	15891.6721(77)
	B_4'	0.28098(5)	0.28020(3)	0.27956(8)	0.27782(8)	0.27652(21)
	r_4'	1.9558(2)	1.9567(1)	1.9571(3)	1.9596(3)	1.9607(7)
	$p_\Delta' + 4q_\Delta'$	0.000264(2)	0.000252(2)	0.000226(6)	0.000176(2)	
A3/2 $v' = 3$	ν_0	15532.8748(22)	15531.1305(12)	15529.4125(17)	15526.0971(20)	15522.9294(22)
	B_3'	0.27998(5)	0.27954(3)	0.27916(6)	0.27792(8)	0.27752(14)
	r_3'	1.9593(2)	1.9590(1)	1.9585(2)	1.9592(3)	1.9572(5)
A3/2 $v' = 4$	ν_0	16116.5304(20)	16114.2296(15)	16111.9705(18)	16107.6036(30)	
	B_4'	0.27859(8)	0.27816(3)	0.27778(7)	0.27655(7)	
	r_4'	1.9642(3)	1.9638(1)	1.9633(2)	1.9641(2)	
X3/2 $v'' = 0$	B_0''	0.31139(6)	0.31086(6)	0.31036(8)	0.30889(10)	0.30842(24)
	r_0''	1.8579(2)	1.8577(2)	1.8574(2)	1.8584(3)	1.8566(7)
	B_1''	0.30870(40)	0.30963(105)	0.30893(32)		
	r_1''	1.8660(12)	1.8639(18)	1.8617(10)		
	$\Delta G_{1/2}''$	691.45(2)	690.80(3)	690.12(1)		

[a]Owing to perturbations, only one component of the C3/2 – X3/2 6-0 band could be fitted. Similarly, perturbations become apparent at higher values of J in the C3/2 – X3/2 5-0 band. Only the low-J transitions were included in the fit reported here. The measured line positions of the A-X 3-0, A-X 4-0, C-X 4-0, and one component of the C-X 6-0 band were simultaneously fitted to extract the ground state constant, B_0''. The C-X 5-1 band was used to extract B_1'' and $\Delta G_{1/2}''$ as described in the text. The bond lengths listed here are obtained from direct inversion of the rotational constants, without any S-uncoupling corrections. S-uncoupling corrections are discussed in the text.

isotopic modification, $^{90}Zr^{19}F$. The spectrum shows a head in the R-branch, with a large number of P lines marching off to lower wavenumbers. A weak Q branch with rapidly diminishing intensity indicates that the transition has $\Delta\Omega = 0$, as do all of the bands that were investigated in this study. The assigned lines fit very well to the simple formula

$$\nu = \nu_0 + B'J'(J'+1) - B''J''(J''+1), \tag{3.4}$$

indicating that there is no observable lambda doubling for either the upper or lower state in this band. Further, the first lines of P(2.5), Q(1.5), and R(1.5) demonstrate that $\Omega' = \Omega'' = 3/2$. A scan over the 4-0 band shows a very similar spectrum as that displayed in Figure 4.

Simulation of this spectrum requires a surprisingly high temperature, roughly 100 K. This is unusual for our supersonic expansion source. The point of vaporization in our source is about 1 cm upstream of the final expansion orifice, so normally the molecules produced in our source are exposed to a large number of collisions prior to and during expansion, resulting in cold molecules (10-20 K). The high rotational temperature observed in this case suggests that ZrF molecules that form close to the point of ablation go on to react further, producing larger species such as ZrF_2 or ZrFCl, which are also detected in the mass spectrum in significant quantities. The ZrF molecules that we detect are likely formed just as the gases are expanding into vacuum, limiting the amount of cooling that they experience, leading to the high rotational temperatures that are observed. This possibility also accounts for the significant population in $v'' = 1$ as well.

2. Rotationally resolved spectra of the B-X system

Rotationally resolved studies of the B-X system have been frustrating due to the fact that all of the bands investigated are strongly perturbed. Although it has been possible to assign rotational lines in the B-X 5-0 band, the $v' = 5$ level shows a large lambda doubling that leads to two R-branch band heads, and a pronounced curvature in the reduced term energy plot. It is simply not possible to extract any meaningful upper state rotational constants from this band. Likewise, the B-X 6-0 band is severely perturbed and could not

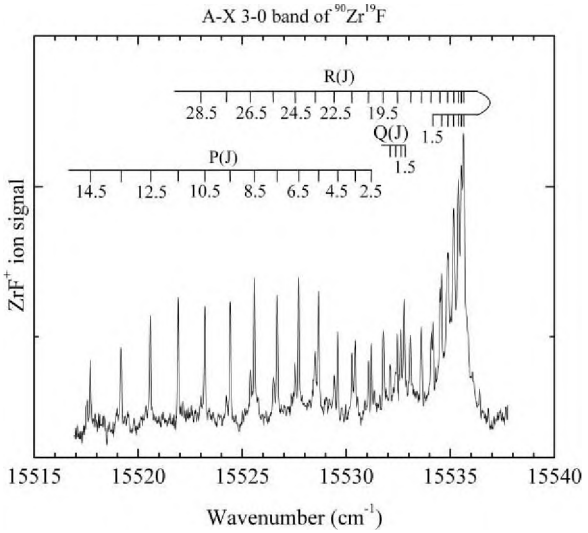

FIG. 4. Rotationally resolved spectrum of the 3-0 band of the A-X system of $^{90}Zr^{19}F$.

be analyzed. Finally, the B-X 7-0 band was examined, and two distinct bands were found for the $^{90}Zr^{19}F$ isotopic modification, separated by only 2.5 cm^{-1}. Although these could both be assigned and fitted, it is doubtful that useful information can be obtained from this analysis. It appears that the B state of ZrF has $\Omega' = 3/2$, although overlapping lines in this perturbed band system makes this conclusion rather tentative. In contrast, the A and C states of ZrF definitely possess $\Omega' = 3/2$.

3. Rotationally resolved spectra of the C3/2-X3/2 system

Rotationally resolved studies of the C-X system were partially successful. The 4-0 band, displayed in Figure 5 for the $^{90}Zr^{19}F$ isotopic modification, is apparently unperturbed except for remote perturbations that lead to lambda doubling, which is evident in the P branch. The spectrum is readily fitted to the form

$$\nu = \nu_0 + B'J'(J'+1) \pm [-1/2(p'_\Delta + 4q'_\Delta)]\,(J'-1/2) \times (J'+1/2)\,(J'+3/2) - B''J''(J''+1), \quad (3.5)$$

for $^{90}Zr^{19}F$, $^{91}Zr^{19}F$, $^{92}Zr^{19}F$, and $^{94}Zr^{19}F$ and displays a smooth, monotonic decrease in the magnitude of the lambda doubling ($p_\Delta' + 4\,q_\Delta'$) with reduced mass. The form of the lambda doubling employed in Eq. (3.5) is valid for a $^2\Delta_{3/2}$ upper state,[61] but requires a redefinition of the constant ($p_\Delta' + 4\,q_\Delta'$) if the upper state is a $^2\Pi_{3/2}$, $^4\Pi_{3/2}$, or $^4\Delta_{3/2}$ state.[61,62] Regardless of the nature of the upper state, however, the first nonvanishing correction due to lambda doubling in an $\Omega = 3/2$ state exhibits the J-dependence given in Eq. (3.5),[61,62] which fits the spectrum well.

The 5-0 and 5-1 bands of the C3/2 – X3/2 system were also investigated, leading to an improved value of $\Delta G_{1/2}''$. These bands exhibit perturbations that prevent them from being fitted to the form of Eq. (3.5). Nevertheless, lines have been identified and the differences between corresponding lines allow $\Delta G_{1/2}''$ to be determined via the equation

$$\nu(C5-0,\ J' \leftarrow J'') - \nu(C5-1,\ J' \leftarrow J'') = \Delta G''_{1/2} + (B_1'' - B_0'')\,J''(J''+1). \quad (3.6)$$

Using Eq. (3.6), the measured differences between corresponding rotational lines were fitted as a linear function of $J''(J''+1)$, allowing values of $\Delta G_{1/2}''$ and (B_1''- B_0'') to be extracted from the data. The resulting values of $\Delta G_{1/2}''$ for $^{90}Zr^{19}F$, $^{91}Zr^{19}F$, and $^{92}Zr^{19}F$ are 691.45(2), 690.83(1), and 690.12(1) cm^{-1}, respectively. These are slightly larger than the values estimated from the measured band heads using the band difference histogram method. The derived values of B_1'' and r_1'' are provided in Table III.

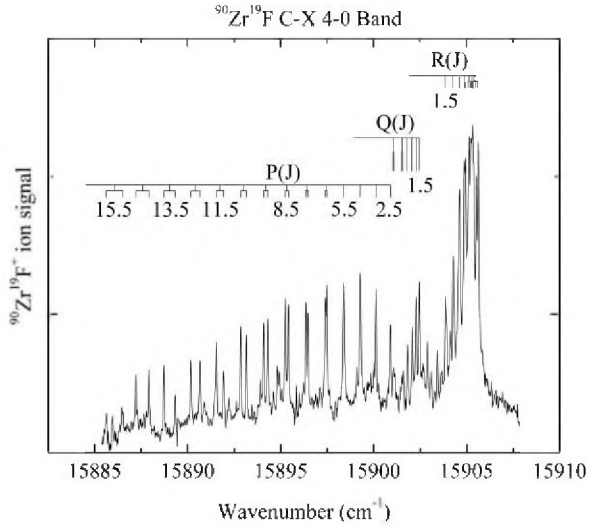

FIG. 5. Rotationally resolved spectrum of the 4-0 band of the C-X system of $^{90}Zr^{19}F$. Lambda doubling is evident in the P-branch, but less obvious in the R-branch.

IV. DISCUSSION

While it is satisfying that this investigation has successfully determined the bond length and vibrational frequency of the ZrF ground state, it is unfortunate that the ground electronic configuration and term cannot be clearly identified by the spectroscopic measurements alone. Owing to the high electron affinity of fluorine (3.399 eV)[63] and the low ionization energy of zirconium (6.634 eV),[64] the molecule is certainly ionic in its low energy states, arising from a combination of $Zr^+ + F^-$. While the F^- anion is a closed-shell, $2p^6$, ^1S_g species, the Zr^+ ion has low-lying states arising from the $4d^3$, $4d^2 5s^1$, and $4d^1 5s^2$ configurations. The lowest energy levels in each of these configurations are $^4F_{3/2g}$, $^4F_{3/2g}$, and $^2D_{3/2g}$, lying at 2572, 0, and 14 299 cm^{-1}, respectively.[55] Further, the $4d^3$, $4d^2 5s^1$, and $4d^1 5s^2$ configurations lead to 29, 21, and 3 molecular terms described by S and Λ, respectively, which in turn generate 60, 45, and 5 distinct doubly-degenerate spin-orbit levels labeled by S, Λ, and Ω. Thus, the electronic structure of ZrF is rather complicated.

In the isovalent TiF, TiCl, and TiBr molecules, it is now clear that the ground state is the $3\sigma^1 1\delta^1 2\pi^1$, $^4\Phi_{3/2}$ level that correlates to the $3d\ ^2 4s^1$, ^4F_g ground term of the Ti^+ ion.[14,15,49,65–70] In the 5*d* analogs, HfF and HfCl, on the other hand, the ground state is the $3\sigma^2 1\delta^1$, $^2\Delta_{3/2}$ level that correlates to the $5d^1 6s^2$, ^2D_g ground term of Hf^+, with a significant contribution from the $5d^2 6s^1$ configuration.[7,71,72] The zirconium halides, however, lie in an intermediate position between these two clear-cut cases. In ZrCl, careful *ab initio* calculations place the $^2\Delta$ term only 330–760 cm^{-1} below the $^4\Phi$ term.[7,49] This separation is expected to narrow when spin-orbit interaction is taken into account, because the $^2\Delta_{3/2}$ level has a first order spin-orbit correction, calculated using numerical Hartree-Fock methods to evaluate ζ_{4d} for the $4d^1 5s^2$, ^2D_g term of Zr^+,[73] of $-\zeta_{4d}(Zr^+,\ 4d^1 5s^2,\ ^2D) \approx -460$ cm^{-1}, while the $^4\Phi_{3/2}$ level has a first-order spin-orbit energy correction of $-3/2\ \zeta_{4d}(Zr^+,\ 4d\ ^2 5s^1,\ ^4F) \approx -598$ cm^{-1}. Thus, the spin-orbit interaction may be expected to reduce the separation between these two states by roughly 138 cm^{-1}. Although it is now thought that the ZrCl ground state is of $^2\Delta_{3/2}$ symmetry,[7] this is a very close call. Further complicating matters is the fact that both candidates for the ground state of ZrCl, $3\sigma^1 1\delta^1 2\pi^1$, $^4\Phi_{3/2}$, and $3\sigma^2 1\delta^1$, $^2\Delta_{3/2}$ have $\Omega = 3/2$, making them difficult to distinguish

unless the higher lying spin components are populated and resolved. Indeed, if the $^2\Delta_{3/2}$ and $^4\Phi_{3/2}$ states are sufficiently close in energy, spin-orbit mixing of these levels may render the S and Λ labels meaningless.

A similar pattern of low-lying states is expected in ZrF, with a close competition between the $3\sigma^1 1\delta^1 2\pi^1$, $^4\Phi_{3/2}$ and $3\sigma^2 1\delta^1$, $^2\Delta_{3/2}$ states as to which emerges as the ground state. Although these two states are quite close in energy in ZrCl, it is reasonable to expect the $^2\Delta_{3/2}$ level to emerge clearly as the ground state in ZrF. As has been pointed out by Field, the transition metal halides can be well-understood by a ligand field model in which the metal-centered orbitals undergo an energy shift given by[25]

$$\Delta E(n\ell\lambda) = B_0^0(n\ell) + B_0^2(n\ell)C_0^2(n\ell\lambda) + B_0^4(n\ell)C_0^4(n\ell\lambda), \tag{4.1}$$

where the B-factors are radial integrals given by

$$B_0^k(n\ell) = Z_L e^2\left[r_e^{-(k+1)}\int_0^{r_e} R_{n\ell}R_{n\ell}r^{k+2}dr + r_e^k\int_{r_e}^{\infty} R_{n\ell}R_{n\ell}r^{-k+1}dr\right] \tag{4.2}$$

and the C-factors are angular integrals that are readily expressed in terms of 3-j symbols:

$$C_0^k(n\ell\lambda) = (-1)^\lambda(2\ell+1)\begin{pmatrix} l & k & l \\ -\lambda & 0 & \lambda\end{pmatrix}\begin{pmatrix} l & k & l \\ 0 & 0 & 0\end{pmatrix}. \tag{4.3}$$

In expression (4.2), Z_L is the magnitude of the negative charge on the ligand (+1 for the case of ZrF or ZrCl) and r_e is the bond length of the molecule. In this simplified discussion, off-diagonal portions of the ligand-field Hamiltonian are ignored, as they are irrelevant to the main point. In expression (4.1), the $B_0^0(n\ell)$ term causes a destabilization of all of the metal-based orbitals as the F^- ion is brought in from infinity, while the remaining terms involving $B_0^2(n\ell)$ and $B_0^4(n\ell)$ cause a splitting of the orbitals on the basis of λ. Further, the $B_0^0(n\ell)$ term increases the energy of the 4*d* orbitals more than it does the 5*s* orbital, effectively because the 5*s* orbital extends further beyond the location of the ligand. Thus, placement of electrons in the 5*s* orbital allows the negatively charged fluoride ion to feel more of the underlying charge of the Zr^+ ion, thereby reducing the net upward shift of the energy of the 5*s* orbital. More generally, diffuse orbitals are destabilized less severely than are compact orbitals; thus, occupation of the more diffuse 5*s* orbital is favored as the negatively charged ligand is brought up to the Zr^+ ion.

As is evident in Eq. (4.2), the ligand field parameters, B_k^0, depend on the bond length, r_e, becoming smaller as the ligand is pulled out to longer distances. Thus, the increase in bond length that occurs as one moves from F^- to Cl^-, Br^-, and I^- causes the ligand field interactions to decrease, a fact that is well-known in inorganic chemistry and has been nicely documented in the YF, YCl, YBr, YI series.[74,75] To attempt to quantify this effect, we have used numerical Hartree-Fock methods to calculate the radial wavefunctions, $R_{4d}(r)$ and $R_{5s}(r)$, for the Zr^+ ion in its $4d^1 5s^2$, ^2D_g and $4d^2 5s^1$, ^4F_g configurations.[73] With these wavefunctions in hand, it is straightforward to compute the values of the ligand-field parameters $B_0^k(4d)$ and $B_0^k(5s)$. To a first order approximation, the effect of the ligand on the energies of these configurations can be estimated by combining the $B_0^k(n\ell)$ terms for the three relevant electrons, weighted by the values of the $C_0^k(n\ell\lambda)$ coefficients as indicated in Eq. (4.1). The result for ZrF, using a value of r_e in Eq. (4.2) given by the measured bond length of 1.858 Å, is a predicted stabilization of the $4d^1 5s^2$, $3\sigma^2 1\delta^1$, $^2\Delta$ term over the $4d^2 5s^1$, $3\sigma^1 1\delta^1 2\pi^1$, $^4\Phi$ term by 4533 cm^{-1}. When the same calculation is performed for ZrCl using the measured bond length of 2.284 Å, the predicted relative stabilization of the $4d^1 5s^2$, $3\sigma^2 1\delta^1$, $^2\Delta$ term is only 1699 cm^{-1}. Subtracting these values, we calculate that the $3\sigma^2 1\delta^1$, $^2\Delta_{3/2}$ state is approximately 2834 cm^{-1} further below the $3\sigma^1 1\delta^1 2\pi^1$, $^4\Phi_{3/2}$ state in ZrF than it is in ZrCl. On this basis it seems likely that the ground state of ZrF is the $3\sigma^2 1\delta^1$, $^2\Delta_{3/2}$ state that is already assigned as the ground state in ZrCl.[7]

While the ligand field calculation outlined above provides some insight into the electronic structure of ZrF, it is difficult to carry this further into a full calculation of the expected electronic states of the molecule. To properly treat this system using ligand field methods, it would be necessary to include the effects of the off-diagonal $B_0^2(4d, 5s)$ term, which is quite large (15 000 cm^{-1} in ZrCl; 22 000 cm^{-1} in ZrF). This term causes mixing of the $4d\sigma$ and $5s\sigma$ orbitals, and is quite important due to the near-degeneracy of these orbitals. Secondly, a proper LFT calculation of the expected state ordering in ZrF would require adjustment of the asymptotic energies of the various states to reproduce the measured Zr^+ energy levels.[55,76] This is straightforward in principle, but is complicated by the strong configuration interaction that is known to occur between terms belonging to the $4d^3$, $4d^2 5s^1$, and $4d^1 5s^2$ configurations.[77] The strong configurational mixing that occurs in the isolated Zr^+ ion complicates the use of ligand-field methods to predict the electronic structure of the ZrF and ZrCl molecules, because a detailed understanding of the atomic states is required before this method can be applied. Indeed, the advantage of the ligand field method is that it is based on already well-understood atomic energy levels; if these levels are themselves poorly understood or not easily described, application of ligand field methods becomes more problematic.

The very recent IC-MRCI investigation of ZrF is in agreement with these ideas, placing the X $^2\Delta$ ground term 2383 cm^{-1} below the a $^4\Sigma^-$ term and 4179 cm^{-1} below the b $^4\Phi$ term.[3] These separations are significantly greater than those obtained in a similar calculation on ZrCl, 963 cm^{-1} and 616 cm^{-1}, respectively.[7] Thus, the combination of experimental data and computational investigations has clearly determined the ground state of ZrF to be $3\sigma^2\ 1\delta^1$, $^2\Delta$. The IC-MRCI study of ZrF also predicts the first and second excited $^2\Delta$ terms to lie in the 14 000 – 18 000 cm^{-1} range. As these are the only possible Hund's case (a) terms that can provide a source of oscillator strength for a parallel transition from a $^2\Delta$ ground term, and this is the region probed in the present study, it is likely that these two $^2\Delta$ terms account for two of our observed band systems. The remaining band system is likely a spin-forbidden transition that is made observable by spin-orbit mixing with the 2 $^2\Delta$ and 3 $^2\Delta$ terms that lie in

this region. Given that the A3/2 and C3/2 states lie quite close in energy ($\Delta T_0 \approx 106$ cm^{-1}) and have similar bond lengths ($\Delta r_4 \approx 0.008$ Å), and that the spin orbit parameter for Zr 4*d* orbitals is larger than their separation ($\zeta_{Zr}(4d) \approx 430$ cm^{-1}), it seems likely that these states are strong mixtures of an electronically bright $^2\Delta$ state and a dark state, probably quartet in character. If so, these states should exhibit fluorescence to both doublet and quartet states in good yield.

V. CONCLUSION

Resonant two-photon ionization spectroscopy has been applied to jet-cooled ZrF, providing spectroscopic data in the 760-555 nm range that complements a previous investigation in the 420-470 nm range. The ground state of the most abundant isotopic modification, $^{90}Zr^{19}F$, has been shown to have $\Omega = 3/2$, $\Delta G''_{1/2} = 691.45(2)$ cm^{-1}, and $r''_e = 1.854(1)$ Å. Three band systems have been identified in the 760 – 555 nm wavelength range, along with a large number of unassigned bands. All three of the band systems appear to have upper states with $\Omega = 3/2$, and many of the bands that have been rotationally resolved show evidence of perturbations. Based on a comparison to ZrCl and a consideration of ligand field effects, it is argued that the ground state of the molecule is $3\sigma^2\,1\delta^1$, $^2\Delta_{3/2}$.

Vibrationally resolved spectra of ZrCl are also reported over the range 760 – 555 nm, and four new band systems are reported for this molecule, along with a large number of unassigned bands.

ACKNOWLEDGMENTS

The authors thank the U.S. Department of Energy for support of this research under Grant No. DE-FG03-01ER15176.

[1] L. A. Kaledin, J. E. McCord, M. C. Heaven, and R. F. Barrow, J. Mol. Spectrosc. **169**, 253 (1995).
[2] J. W. H. Leung, J. Dai, and A. S. C. Cheung, J. Mol. Spectrosc. **207**, 124 (2001).
[3] S. Soorkia, N. Shafizadeh, A. Gaveau, C. Pothier, J. M. Mestdagh, B. Soep, J. Lievin, and R. W. Field, J. Phys. Chem. A (in press).
[4] K. J. Jordan, R. H. Lipson, N. A. McDonald, and D. S. Yang, Chem. Phys. Lett. **193**, 499 (1992).
[5] R. S. Ram and P. F. Bernath, J. Mol. Spectrosc. **186**, 335 (1997).
[6] R. S. Ram and P. F. Bernath, J. Mol. Spectrosc. **196**, 235 (1999).
[7] R. S. Ram, A. G. Adam, W. Sha, A. Tsouli, J. Lievin, and P. F. Bernath, J. Chem. Phys. **114**, 3977 (2001).
[8] R. S. Ram, N. Rinskopf, J. Lievin, and P. F. Bernath, J. Mol. Spectrosc. **228**, 544 (2004).
[9] T. C. Steimle, W. L. Virgo, and T. Ma, J. Chem. Phys. **124**, 024309/1-/7 (2006).
[10] R. Li, R. H. Jensen, W. J. Balfour, S. A. Shepard, and A. G. Adam, J. Chem. Phys. **121**, 2591 (2004).
[11] S. A. Shepard, A. G. Adam, R. Li, and W. J. Balfour, J. Mol. Spectrosc. **234**, 204 (2005).
[12] R. M. Clements and R. F. Barrow, Chem. Commun. 27 (1968).
[13] G. J. Stueber, M. Foltin, and E. R. Bernstein, J. Chem. Phys. **109**, 9831 (1998).
[14] R. S. Ram, J. R. D. Peers, Y. Teng, A. G. Adam, A. Muntianu, P. F. Bernath, and S. P. Davis, J. Mol. Spectrosc. **184**, 186 (1997).
[15] R. S. Ram and P. F. Bernath, J. Mol. Spectrosc. **186**, 113 (1997).
[16] S. M. Kermode and J. M. Brown, J. Mol. Spectrosc. **207**, 161 (2001).
[17] R. S. Ram, P. F. Bernath, and S. P. Davis, J. Mol. Spectrosc. **173**, 158 (1995).
[18] T. Hirao, B. Pinchemel, and P. F. Bernath, J. Mol. Spectrosc. **219**, 119 (2003).
[19] J. F. Harrison, Chem. Rev. **100**, 679 (2000).
[20] C. Koukounas and A. Mavridis, J. Phys. Chem. A **112**, 11235 (2008).
[21] C. Koukounas, S. Kardahakis, and A. Mavridis, J. Chem. Phys. **120**, 11500 (2004).
[22] B. Kharat, S. B. Deshmukh, and A. Chaudhari, Int. J. Quantum Chem. **109**, 1103 (2009).
[23] L. Cheng, M. Y. Wang, Z. J. Wu, and Z. M. Su, J. Comput. Chem. **28**, 2190 (2007).
[24] P. E. M. Siegbahn, Theor. Chim. Acta **86**, 219 (1993).
[25] R. W. Field, Ber. Bunsenges. Phys. Chem. **86**, 771 (1982).
[26] P. Carette, C. Dufour, and B. Pinchemel, J. Mol. Spectrosc. **161**, 323 (1993).
[27] A. L. Kaledin, M. C. Heaven, R. W. Field, and L. A. Kaledin, J. Mol. Spectrosc. **179**, 310 (1996).
[28] L. A. Kaledin, A. L. Kaledin, and M. C. Heaven, J. Mol. Spectrosc. **179**, 246 (1996).
[29] J. Ren, M. H. Whangbo, D. Dai, and L. Li, J. Chem. Phys. **108**, 8479 (1998).
[30] J. Schamps, M. Bencheikh, J.-C. Barthelat, and R. W. Field, J. Chem. Phys. **103**, 8004 (1995).
[31] L. A. Kaledin, M. G. Erickson, and M. C. Heaven, J. Mol. Spectrosc. **165**, 323 (1994).
[32] L. A. Kaledin, J. E. McCord, and M. C. Heaven, J. Mol. Spectrosc. **170**, 166 (1995).
[33] L. A. Kaledin, J. E. McCord, and M. C. Heaven, J. Mol. Spectrosc. **164**, 27 (1994).
[34] S. F. Rice, H. Martin, and R. W. Field, J. Chem. Phys. **82**, 5023 (1985).
[35] D. P. Baldwin, E. J. Hill, and R. W. Field, J. Am. Chem. Soc. **112**, 9156 (1990).
[36] Z. J. Jakubek and R. W. Field, J. Chem. Phys. **98**, 6574 (1993).
[37] L. A. Kaledin, J. E. McCord, and M. C. Heaven, J. Mol. Spectrosc. **173**, 499 (1995).
[38] L. A. Kaledin, J. E. McCord, and M. C. Heaven, J. Mol. Spectrosc. **173**, 37 (1995).
[39] L. A. Kaledin and M. C. Heaven, J. Chem. Phys. **107**, 7020 (1997).
[40] C. Focsa, M. Bencheikh, and L. G. M. Pettersson, J. Phys. B At., Mol. Opt. Phys. **31**, 2857 (1998).
[41] M. Bencheikh, R. Koivisto, O. Launila, and J. P. Flament, J. Chem. Phys. **106**, 6231 (1997).
[42] M. Bencheikh, J. Phys. B At., Mol. Opt. Phys. **30**, L137 (1997).
[43] M. Bencheikh, J. Mol. Spectrosc. **183**, 419 (1997).
[44] M. Afaf, Proc. Phys. Soc., London **63A**, 544 (1950).
[45] P. K. Carroll and P. J. Daly, Proc. Phys. Soc., London **70A**, 549 (1957).
[46] D. L. Hildenbrand and K. H. Lau, J. Chem. Phys. **107**, 6349 (1997).
[47] P. K. Carroll and P. J. Daly, Proc. R. Irish Acad., Sect. A: Math. Phys. Sci. **61A**, 101 (1961).
[48] J. G. Phillips, S. P. Davis, and D. C. Galehouse, Astrophys. J., Suppl. Ser. **43**, 417 (1980).
[49] Y. Sakai, K. Mogi, and E. Miyoshi, J. Chem. Phys. **111**, 3989 (1999).
[50] R. Nagarajan and M. D. Morse, J. Chem. Phys. **126**, 144309/1-/6 (2007).
[51] D. J. Brugh and M. D. Morse, J. Chem. Phys. **107**, 9772 (1997).
[52] W. C. Wiley and I. H. McLaren, Rev. Sci. Instrum. **26**, 1150 (1955).
[53] B. A. Mamyrin, V. I. Karataev, D. V. Shmikk, and V. A. Zagulin, Zh. Eksp. Teor. Fiz. **64**, 82 (1973).
[54] J. K. Bates and T. M. Dunn, Can. J. Phys. **54**, 1216 (1976).
[55] C. E. Moore, *Atomic Energy Levels*, Natl. Bur. Stand. U.S. Circ. No. 467 ed. (U.S. Government Printing Office, Washington, D.C., 1971).
[56] S. Gerstenkorn and P. Luc, *Atlas du Spectre d'Absorption de la Molécule d'Iode entre 14,800-20,000 cm^{-1}* (CNRS, Paris, 1978).
[57] S. Gerstenkorn and P. Luc, Rev. Phys. Appl. **14**, 791–4 (1979).
[58] P. R. Bevington, *Data Reduction and Error Analysis for the Physical Sciences* (McGraw-Hill, New York, 1969).
[59] G. Herzberg, *Molecular Spectra and Molecular Structure I. Spectra of Diatomic Molecules*, 2nd ed. (Van Nostrand Reinhold, New York, 1950).
[60] See supplementary material at http://dx.doi.org/10.1063/1.3608055 for 69 pages of band positions, isotope shift measurements, plotted spectra, rotational line positions, rotational fits, and associated information for ZrCl and ZrF.
[61] J. M. Brown, A. S.-C. Cheung, and A. J. Merer, J. Mol. Spectrosc. **124**, 464 (1987).
[62] J. M. Brown and A. J. Merer, J. Mol. Spectrosc. **74**, 488 (1979).
[63] H. Hotop and W. C. Lineberger, J. Phys. Chem. Ref. Data **14**, 731 (1985).

[64]P. A. Hackett, M. R. Humphries, S. A. Mitchell, and D. M. Rayner, J. Chem. Phys. **85**, 3194 (1986).
[65]T. Imajo, Y. Kobayashi, Y. Nakashima, K. Tanaka, and T. Tanaka, J. Mol. Spectrosc. **230**, 139 (2005).
[66]R. S. Ram and P. F. Bernath, J. Mol. Spectrosc. **231**, 165 (2005).
[67]T. Imajo, D. Wang, K. Tanaka, and T. Tanaka, J. Mol. Spectrosc. **203**, 216 (2000).
[68]A. Maeda, T. Hirao, P. F. Bernath, and T. Amano, J. Mol. Spectrosc. **210**, 250 (2001).
[69]A. I. Boldyrev and J. Simons, J. Mol. Spectrosc. **188**, 138 (1998).
[70]A. G. Adam, W. S. Hopkins, W. Sha, and D. W. Tokaryk, J. Mol. Spectrosc. **236**, 42 (2006).
[71]A. G. Adam, W. S. Hopkins, and D. W. Tokaryk, J. Mol. Spectrosc. **225**, 1 (2004).
[72]R. S. Ram, A. G. Adam, A. Tsouli, J. Lievin, and P. F. Bernath, J. Mol. Spectrosc. **202**, 116 (2000).
[73]C. F. Fischer, *The Hartree-Fock Method for Atoms* (John Wiley & Sons, New York, 1977).
[74]J. E. Huheey, *Inorganic Chemistry* (Harper & Row, New York, 1983).
[75]J. Ye, H. F. Pang, and A. S. C. Cheung, Chem. Phys. Lett. **442**, 251 (2007).
[76]C. C. Kiess, J. Opt. Soc. Am. **43**, 1024 (1953).
[77]L. Young, C. A. Kurtz, D. R. Beck, and D. Datta, Phys. Rev. A **48**, 173 (1993).